

Electrochemical investigation of the anode processes in LiF–NdF₃ melt with low oxygen content

Chen-ming Fan, Shi-zhe Liu, Jing-jiu Gu, Shi-you Guan, Jin-hua Zhao, and Bing Li

Cite this article as:

Chen-ming Fan, Shi-zhe Liu, Jing-jiu Gu, Shi-you Guan, Jin-hua Zhao, and Bing Li, Electrochemical investigation of the anode processes in LiF–NdF₃ melt with low oxygen content, *Int. J. Miner. Metall. Mater.*, 28(2021), No. 3, pp. 398-403. <https://doi.org/10.1007/s12613-020-2010-7>

View the article online at [SpringerLink](#) or [IJMMM Webpage](#).

Articles you may be interested in

Jian-long Guo, Yan-ping Bao, and Min Wang, [Cleanliness of Ti-bearing Al-killed ultra-low-carbon steel during different heating processes](#), *Int. J. Miner. Metall. Mater.*, 24(2017), No. 12, pp. 1370-1378. <https://doi.org/10.1007/s12613-017-1529-8>

Shu-mei Chen, Chun-fa Liao, Jue-yuan Lin, Bo-qing Cai, Xu Wang, and Yun-fen Jiao, [Electrical conductivity of molten LiF–DyF₃–Dy₂O₃–Cu₂O system for Dy–Cu intermediate alloy production](#), *Int. J. Miner. Metall. Mater.*, 26(2019), No. 6, pp. 701-709. <https://doi.org/10.1007/s12613-019-1775-z>

Qing Yuan, Guang Xu, Wei-cheng Liang, Bei He, and Ming-xing Zhou, [Effects of oxygen content on the oxidation process of Si-containing steel during anisothermal heating](#), *Int. J. Miner. Metall. Mater.*, 25(2018), No. 2, pp. 164-172. <https://doi.org/10.1007/s12613-018-1559-x>

Hong-xiang Li, Shi-kai Qin, Ying-zhong Ma, Jian Wang, Yun-jin Liu, and Ji-shan Zhang, [Effects of Zn content on the microstructure and the mechanical and corrosion properties of as-cast low-alloyed Mg–Zn–Ca alloys](#), *Int. J. Miner. Metall. Mater.*, 25(2018), No. 7, pp. 800-809. <https://doi.org/10.1007/s12613-018-1628-1>

Tapan Sarkar, Ajit Kumar Pramanick, Tapan Kumar Pal, and Akshay Kumar Pramanick, [Development of a new coated electrode with low nickel content for welding ductile iron and its response to austempering](#), *Int. J. Miner. Metall. Mater.*, 25(2018), No. 9, pp. 1090-1103. <https://doi.org/10.1007/s12613-018-1660-1>

Jian-fang Lü, Zhe-nan Jin, Hong-ying Yang, Lin-lin Tong, Guo-bao Chen, and Fa-xin Xiao, [Effect of the CaO/SiO₂ mass ratio and FeO content on the viscosity of CaO–SiO₂–“FeO”–12wt%ZnO–3wt%Al₂O₃ slags](#), *Int. J. Miner. Metall. Mater.*, 24(2017), No. 7, pp. 756-767. <https://doi.org/10.1007/s12613-017-1459-5>



IJMMM WeChat



QQ author group

Electrochemical investigation of the anode processes in LiF–NdF₃ melt with low oxygen content

Chen-ming Fan¹, Shi-zhe Liu¹, Jing-jiu Gu¹, Shi-you Guan², Jin-hua Zhao³, and Bing Li¹

1) School of Mechanical and Power Engineering, East China University of Science and Technology, Shanghai 200237, China

2) Institute for Sustainable Energy, College of Sciences, Shanghai University, Shanghai 200444, China

3) Collaborative Innovation Center of Clean Energy, Longyan University, Longyan 364012, China

(Received: 4 December 2019; revised: 6 February 2020; accepted: 10 February 2020)

Abstract: The oxidation of oxygen ions and the generation of an anode effect at a low oxygen content of 150 mg/kg were discussed in this paper. Cyclic voltammetry and square-wave voltammetry tests were conducted to explore the anodic processes of LiF–NdF₃ melt after a lengthy period of pre-electrolysis purification at 1000°C (during which the oxygen content reduced from 413 to 150 mg/kg). The oxidation process of oxygen ions was found to have two stages: oxidation product adsorption and CO/CO₂ gas evolution. The adsorption stage was controlled by diffusion, whereas the gas evolution was controlled by the electrochemical reaction. In comparison with oxygen content of 413 mg/kg, the decrease in the amplitude of the current at low oxygen content of 150 mg/kg was much gentler during the forward scanning process when the anode effect occurred. Fluorine-ion oxidation peaks that occurred at about 4.2 V vs. Li/Li⁺ could be clearly observed in the reverse scanning processes, in which fluorine ions were oxidized and perfluorocarbons were produced, which resulted in an anode effect.

Keywords: LiF–NdF₃ melt; neodymium electrowinning; low oxygen content; anode processes

1. Introduction

Neodymium, a very typical rare earth element, is widely used in the field of permanent magnet and nonferrous metal modification [1–2]. The most prevalent method used to produce neodymium metal is molten salt electrolysis, which is suitable for mass production due to its continuous operation process. In modern industry, a fluoride–oxide molten salt media is the most commonly used electrolyte system for neodymium electrowinning because it has been shown to have a lower hygroscopicity and higher current efficiency than chloride electrolytes [3–6]. However, in the fluoride–oxide electrolysis process, the graphite anode can cause serious problems due to the formation of perfluorocarbons (PFCs) and the occurrence of an anode effect. Perfluorocarbons that are mainly composed of CF₄ and C₂F₆ are typical greenhouse gases, and their emission must be strictly controlled to protect the environment.

To eliminate the generation of PFCs, it is necessary to understand the mechanism of PFC generation. Many researchers [7–9] have studied the anode effect and the PFCs generated by aluminum electrolysis conducted in molten fluoride

salts. Although aluminum electrolysis and neodymium electrolysis are both conducted in fluoride molten salts, there is a huge difference between their anode processes. The anode effect of neodymium electrolysis and the composition of the anode gases in LiF–NdF₃ melt have been explored by Wang *et al.* [6] and Vogel and Friedrich [10]. Over the years, our laboratory has explored the anode processes associated with Nd electrowinning from LiF–NdF₃–Nd₂O₃ melt [11].

In this study, we used the LiF–NdF₃ system to conduct long-term pre-electrolysis purification to reduce the oxygen content in the molten salts as much as possible, and studied the anode processes of neodymium electrolysis in the LiF–NdF₃ melt under a condition approaching pure fluoride. Cyclic and square-wave voltammetry tests were conducted to investigate the oxidation processes of oxygen ions and the potential for oxidizing fluoride ions and generating PFCs in a pure fluoride system with a very low oxygen content of about 150 mg/kg.

2. Experimental

A sealed cylindrical stainless-steel reactor with a stainless-

Corresponding authors: Shi-you Guan E-mail: syguan@shu.edu.cn; Jin-hua Zhao E-mail: 82008021@jyun.edu.cn;

Bing Li E-mail: drlibing@163.com, bingli@ecust.edu.cn

© University of Science and Technology Beijing and Springer-Verlag GmbH Germany, part of Springer Nature 2021

steel lid was used in all the electrochemical experiments conducted in this study. LiF (Hebei Yucheng Chemical Co., Ltd., China) and NdF₃ (Xuzhou Jinshi Pengyuan Rare Earth Material Factory, China) were respectively maintained at 400°C for more than 12 h under vacuum to remove moisture and then mixed in the proportions of 30wt% and 70wt% in a vacuum glove box. Well-mixed LiF (60 g) and NdF₃ (140 g) were continuously heated to 1000°C in a graphite crucible at a rate of 5°C/min and kept for 2 h in an argon atmosphere. All the electrochemical experiments were conducted in a three-electrode system in an argon atmosphere, in which a tungsten (W) wire with a diameter (ϕ) of 1 mm was used as the quasi-reference electrode, and then the potential was transferred to an Li/Li⁺ reference electrode according to electrochemical measurements in the literature [12]. A high-purity graphite rod (ϕ 6 mm) and a molybdenum (Mo) wire (ϕ 0.8 mm) were used as the working and counter electrodes, respectively.

The three electrodes were polished and placed into the LiF–NdF₃ melt and then connected to a PAR-STAT2273 (PAR-Ametek Co., Ltd., USA) workstation equipped with a PowerSuite software package for the cyclic voltammetry (CV) and square-wave voltammetry (SWV) tests.

3. Results and discussion

3.1. Cyclic voltammetry

CV tests were conducted to record the electrochemical processes on a graphite anode in the molten LiF–NdF₃

(30wt%/70wt%) melt at 1000°C. Fig. 1(a) shows the cyclic voltammograms obtained by forward scanning from an open-circuit potential to 5.5 V vs. Li/Li⁺ before (curve 1) and after (curve 2) 5 h of pre-electrolysis purification. In curve 1, the oxidation current appeared at 1.9 V vs. Li/Li⁺ and peaked at 2.5 V vs. Li/Li⁺ (peak A in Fig. 1(a)), with a peak current density of 0.080 A/cm². These results confirmed those of our previous experiments that involved the oxidation of oxygen ions [11]. Despite the lengthy drying and pre-melting treatments, the system still contained a certain amount of impurity, i.e., oxygen ions (oxygen content: 413 mg/kg). After 5 h of pre-electrolysis purification (oxygen content: 150 mg/kg), it can be clearly observed from Fig. 1(a) that the current density of curve 2 was significantly lower than that before pre-electrolysis. The oxidation current first appeared at 2.3 V vs. Li/Li⁺, which was more positive than that of curve 1, and the peak current density at 2.6 V vs. Li/Li⁺ (peak A' in Fig. 1(a)) was 0.025 A/cm², which was lower than that of curve 1 and indicated a lower oxygen-ion concentration in the melt after pre-electrolysis. It is obvious that the current of curve 1 was smooth up to 2.75 V vs. Li/Li⁺, then fluctuated sharply and rapidly increased to 0.38 A/cm² when the potential exceeded 2.75 V vs. Li/Li⁺. It can be inferred that the smooth current curve reflects the adsorption process of the substances produced by oxygen-ion oxidation on the graphite anode, as expressed in reactions (1) and (2). The violent fluctuation in current curve 1 occurred upon the release of anode gas, including carbon monoxide (CO) and carbon dioxide (CO₂) [6,9–11].

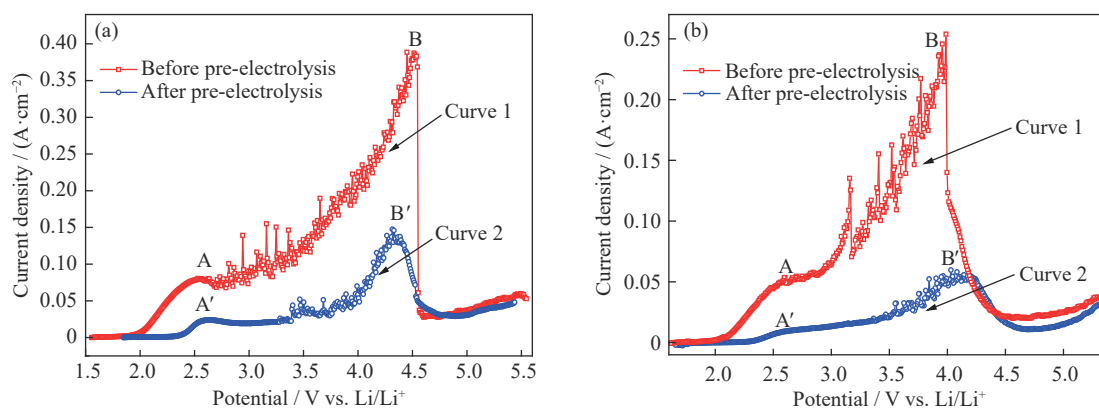


Fig. 1. Cyclic voltammograms recorded on a graphite electrode in LiF–NdF₃ melt at a scan rate of 100 mV/s at 1000°C: (a) forward scan before (curve 1) and after (curve 2) pre-electrolysis; (b) reverse scan before (curve 1) and after (curve 2) pre-electrolysis.



Therefore, the oxidation of the oxygen ions can be said to have two stages, oxidation products adsorption and CO/CO₂ gas evolution, which corresponded to the smooth and fluctuating parts of current curves, respectively. In comparison with the CV results obtained before pre-electrolysis, the CV results obtained after pre-electrolysis had a longer adsorption

time and shorter fluctuation time due to the lower oxygen-ion content in the melt.

Regarding the molten salts prior to pre-electrolysis, when the potential exceeded 4.5 V vs. Li/Li⁺ (peak B in Fig. 1(a)), the current dropped sharply to a very low value of 0.025 A/cm² caused by the anode effect, which was similar to the case in aluminum electrolysis [13]. This effect was due to the generation of a “CF” film on the electrode surface that served

as insulation, which caused the anodic oxidation current to drop sharply to an extremely small value [9,14–15]. The gases produced on a graphite electrode at potentials exceeding 4.5 V vs. Li/Li⁺ have been confirmed by both Wang *et al.* [6] and Zhu and Sadoway [9] to be CF₄ and C₂F₆, as shown in reactions (3) and (4).



After pre-electrolysis purification, the oxidation current began to decrease at 4.3 V vs. Li/Li⁺ (peak B' in Fig. 1(a)), resulting in an anode effect. However, the drop in current was much more gradual than that before pre-electrolysis, and it did not drop to its minimum value until 4.9 V vs. Li/Li⁺. Therefore, we can infer that the oxygen-ion concentration in molten salts has a certain influence on the anode effect. In the reverse scanning process, as shown in Fig. 1(b), the curve after pre-electrolysis was basically the same as that obtained by forward scanning, with current peak occurring at a potential of 4.2 V vs. Li/Li⁺ (peak B' in Fig. 1(b)). We can con-

clude that 4.2 V vs. Li/Li⁺ is a critical potential that generates an anode effect. In another words, 4.2 V vs. Li/Li⁺ is most likely to be the potential at which the oxidation of fluorine ions and the production of perfluorocarbons occurs [9].

Fig. 2(a) shows the forward scanning part of the CVs recorded on a graphite electrode at different scan rates in the 5 h pre-electrolyzed LiF–NdF₃ melt at 1000°C. With increase in the scan rate, the current density of the oxidation peak at 2.5 V vs. Li/Li⁺ increased, and the peak potential moved slightly to a more positive position. In the range of 4.0–4.4 V vs. Li/Li⁺, as the scan rate increased from 10 to 50 mV/s, the density of the oxidation current increased from 0.11 to 0.15 A/cm², whereas the current remained basically unchanged at higher scan rates from 50 to 200 mV/s. As shown in Fig. 2(b), the straight line derived from the current density of peak A in Fig. 2(a) vs. the square root of the scan rate went through the origin. This result indicated that the adsorption of the oxidation products of oxygen ions is controlled by diffusion, whereas the evolution of the CO/CO₂ gas is controlled by the electrochemical reaction.

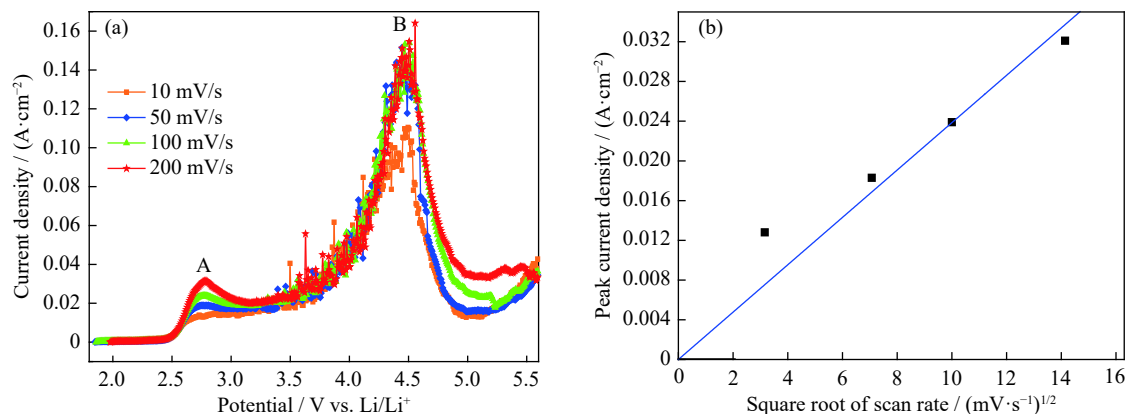


Fig. 2. (a) Forward scanning cyclic voltammograms recorded on a graphite electrode in the 5 h pre-electrolyzed LiF–NdF₃ melt at 1000°C; (b) current density of peak A vs. the square root of the scan rate derived from (a).

Compared with the forward scanning part of the CVs in Fig. 2(a), the current peak at 2.5 V vs. Li/Li⁺ still appeared during the reverse scanning process, but the peak current density of A' remained constant at different scan rates, as shown in Fig. 3(a). In the range of 3.7–4.5 V vs. Li/Li⁺, with increase in the scan rate, the peak current density during the reverse scanning process gradually decreased, and a new peak C' appeared. Meanwhile, with increase in the scan rate, the peak potential of the new current peak C' shifted to a more negative value, whereas the potentials of peak B' near 4.2 V vs. Li/Li⁺ remained basically unchanged. Based on our previous judgment, we consider that the peak at 4.2 V vs. Li/Li⁺ was caused by the oxidation of fluorine ions, and the new peak C' corresponded to the second step in the oxidation of the oxygen ions.

The oxidation peak current density of B' shifted to a more negative value with the increase in the scan rate from 10 to

300 mV/s (Fig. 3(b)). According to studies using other molten salt systems, when an anode effect occurs, the generated PFCs will form a “CF” insulating film on the surface of the graphite electrode, which blocks the electrode reaction and causes a sharp decrease in the current. In the forward scanning process, due to differences in the electrode area and temperature, the critical potential required by the generated PFCs to completely cover the electrode surface and generate an anode effect will differ [11]. During reverse scanning, desorption of PFCs from the surface of the graphite electrode is controlled by the potential alone, but the PFCs departure from the electrode is controlled by diffusion. This leads to obvious oxidation peaks at 4.2 V vs. Li/Li⁺ at different scan rates during reverse scanning due to the fluoride-ion oxidation and formation of PFCs. Thus, we can also prove that the generation of PFCs is strictly controlled by the potential, and 4.2 V vs. Li/Li⁺ is the critical potential for generating PFCs in

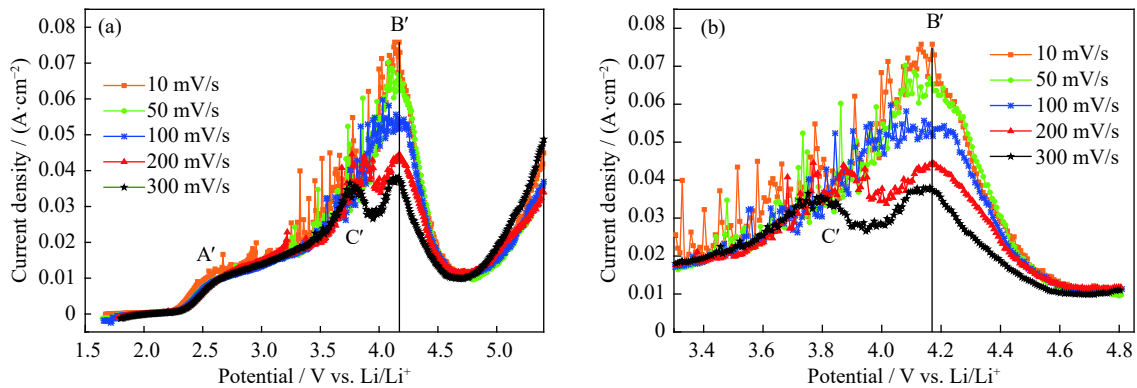


Fig. 3. (a) Reverse scanning cyclic voltammograms recorded on a graphite electrode in pre-electrolyzed LiF–NdF₃ melt at different scan rates at 1000°C; (b) larger and clearer part of (a) from 3.3 to 4.8 V vs. Li/Li⁺.

LiF–NdF₃ melt at 1000°C.

3.2. Square-wave voltammetry

SWV can better clarify the redox process than CV. Here, the conclusions obtained from SWV tests corresponded to and verified those obtained by CV. The square-wave voltammogram in Fig. 4(a) was recorded on a graphite electrode in pre-electrolyzed LiF–NdF₃ melt at a frequency of 25 Hz at 1000°C. We can see clearly in the figure that there was a peak at 2.7 V vs. Li/Li⁺ that corresponded to that of the cyc-

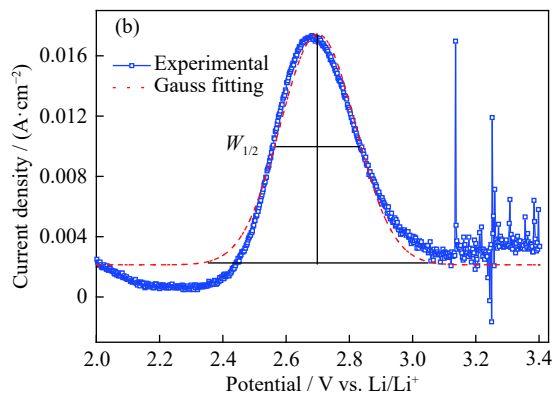
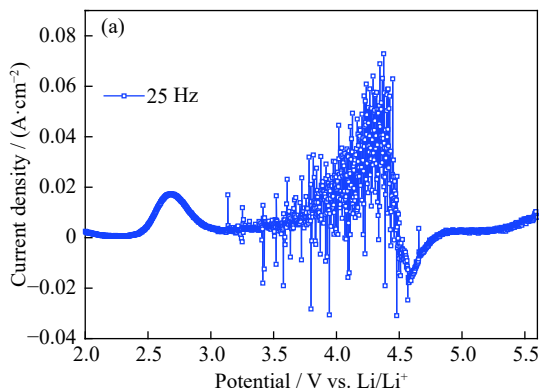


Fig. 4. (a) Square-wave voltammogram recorded on a graphite electrode in pre-electrolyzed LiF–NdF₃ melt (oxygen content: 150 mg/kg) at a frequency of 25 Hz at 1000°C; (b) Gauss fitting of the oxidation peak at 2.7 V vs. Li/Li⁺ in (a).

The number of exchanged electrons was calculated to be 1.63, which verified that the oxidation peak was a two-electron-transfer oxidation process of oxygen ions. Subsequently, due to the release of gas, the square-wave voltammogram also fluctuated violently. This is consistent with the previous conclusion that the oxygen-ion oxidation process had two stages. Although the curve fluctuated wildly, the sharp drop of the current at 4.2 V vs. Li/Li⁺ was obvious, and it reached a minimum value at around 4.6 V vs. Li/Li⁺ before rising. This phenomenon once again indicated that 4.2 V vs. Li/Li⁺ is the critical potential for the generation of an anode effect in LiF–NdF₃ melt with a low oxygen content at 1000°C.

After 5 h pre-electrolysis of the LiF–NdF₃ melt at 1000°C,

lic voltammogram (peak A' in Fig. 1(b)), which was caused by the oxidation of oxygen ions. The half-peak width ($W_{1/2}$) obtained by a Gauss fitting of the oxidation peak at 2.7 V vs. Li/Li⁺ in Fig. 4(b) was substituted into Eq. (5) below to calculate the number of exchanged electrons [16]:

$$W_{1/2} = 3.52 \frac{RT}{nF} \quad (5)$$

where R is the universal gas constant, T is the absolute temperature in K, n is the number of exchanged electrons, and F is Faraday's constant.

we superimposed the square-wave voltammograms at different frequencies to obtain Fig. 5(a). In the figure, we can see that with the increase in frequency, the peak current at 2.7 V vs. Li/Li⁺ also increased, whereas the square-wave voltammograms in the later potential range of 3.0–5.5 V vs. Li/Li⁺ remained coincident. The relationship between the peak current of the oxygen-ion oxidation and the square root of the frequency in Fig. 5(b) was derived from 2.3–3.1 V vs. Li/Li⁺ in Fig. 5(a). The straight line that went through the origin is consistent with the results obtained from the CV tests. Based on these results, we can infer that the adsorption of oxygen-ion oxidation products is controlled by diffusion, whereas the CO/CO₂ gas evolution is controlled by the electrochemical

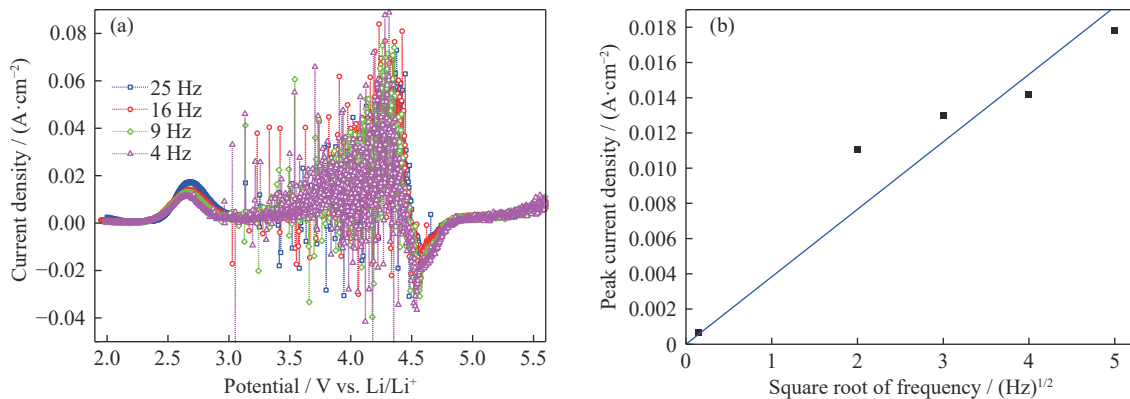


Fig. 5. (a) Square-wave voltammograms recorded on a graphite electrode after 5 h pre-electrolysis LiF–NdF₃ melt at different frequencies at 1000°C; (b) peak current of oxygen-ion oxidation vs. the square root of frequency derived from 2.3–3.1 V vs. Li/Li⁺ in (a).

reaction.

3.3. Special situation after long period of pre-electrolysis

During the experiment, we observed that an interesting phenomenon in the cyclic voltammograms obtained in the LiF–NdF₃ melt with a lower oxygen content (oxygen content: <150 mg/kg) after a lengthy pre-electrolysis sometimes occurred, as shown in Fig. 6. Figs. 6(a) and 6(b) respectively correspond to the curves obtained at scan rates of 100 and

300 mV/s. In these two figures, two peaks appeared during the adsorption step of the oxygen-ion oxidation during the forward scanning process, whereas one peak remained during the reverse scanning process. The reason for this may be that different complexes had formed in the molten salts and the discharge of oxygen ions became a two-step electron transfer that was affected by the formation of these complexes and correspondingly exhibited two peaks in the resulting cyclic voltammograms.

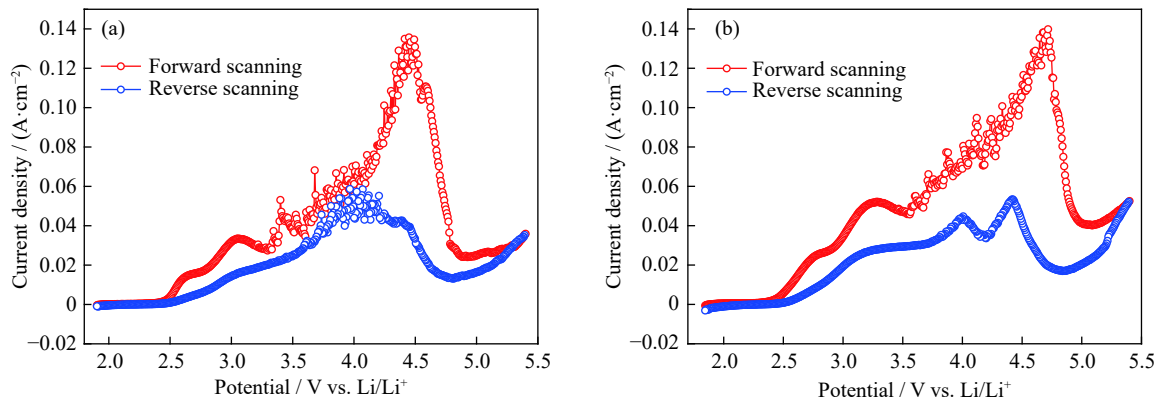


Fig. 6. Cyclic voltammograms recorded on a graphite electrode in pre-electrolyzed LiF–NdF₃ melt with a lower oxygen content (oxygen content: <150 mg/kg) at 1000°C at different scan rates: (a) 100 mV/s; (b) 300 mV/s.

The measured square-wave voltammogram in Fig. 7(a) obtained under a lower oxygen content (oxygen content: <150 mg/kg) was significantly different from that in Fig. 4(a) (oxygen content: 150 mg/kg). In Fig. 7(a), in the range of 2.4–3.4 V vs. Li/Li⁺, two peaks also appeared in the same positions, as compared with Fig. 6(a). According to the calculation, the numbers of exchanged electrons in the redox reaction corresponding to the two peaks was 1.34 and 1.08, respectively, thereby confirming the conclusion that the discharge process of oxygen ion was transformed into a two-step electron transfer, involving one electron at each step.

4. Conclusions

In this paper, we presented the results of CV and SWV

tests to explore the anode processes of LiF–NdF₃ melt after a lengthy period of pre-electrolysis purification (during which the oxygen contents were reduced from 413 to 150 mg/kg).

(1) The oxidation process of oxygen ions had two stages, i.e., oxidation products adsorption and CO/CO₂ gas evolution, which respectively corresponded to the smooth and fluctuating parts of current curves. The adsorption stage was controlled by diffusion, whereas the gas evolution was controlled by the electrochemical reaction.

(2) After pre-electrolysis purification, when an anode effect occurred, the decrease in amplitude of the current was much gentler than that before pre-electrolysis, which indicated that the oxygen ions in the molten salts have a certain impact on the anode effect.

(3) Fluorine-ion oxidation peaks were clearly observed at

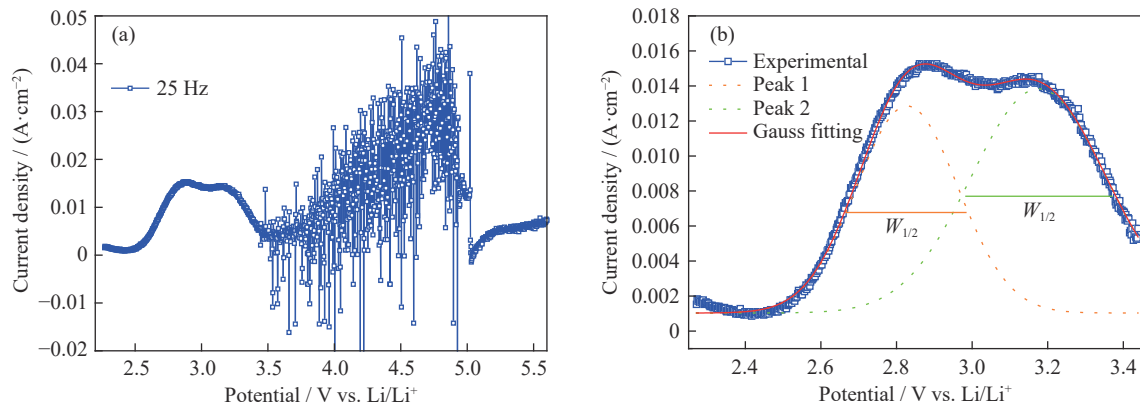


Fig. 7. (a) Square-wave voltammogram recorded on a graphite electrode in pre-electrolyzed LiF–NdF₃ melt with a lower oxygen content (oxygen content: <150 mg/kg) at a frequency of 25 Hz at 1000°C; (b) Gauss fittings of the two peaks between 2.4 and 3.4 V vs. Li/Li⁺ in (a).

about 4.2 V vs. Li/Li⁺ during the reverse scanning processes, with the oxidation of fluorine ions and the production of per-fluorocarbons causing an anode effect. We could conclude that 4.2 V vs. Li/Li⁺ is a critical potential for generating an anode effect.

(4) After a lengthy period of pre-electrolysis, two oxygen-ion oxidation peaks sometimes occurred. Based on our calculations, this was because one electron had transferred at each of the two peaks in the redox reaction. We speculated that the discharge process of oxygen ions was transformed into a two-step electron transfer that was affected by the formation of complexes.

Acknowledgements

This work was financially supported by the National Natural Science Foundation of China (No. 51774145). The “Minjiang Scholar” Program of Department of Education, Fujian Province, China was also acknowledged.

References

- [1] O. Gutfleisch, M.A. Willard, E. Brück, C.H. Chen, S.G. Sankar, and J.P. Liu, Magnetic materials and devices for the 21st century: Stronger, lighter, and more energy efficient, *Adv. Mater.*, 23(2011), No. 7, p. 821.
- [2] A. Hosokawa and K. Takagi, Anisotropic nanocomposite Nd–Fe–B magnets produced by hot deformation with assistance of Nd–Cu, *J. Magn. Magn. Mater.*, 489(2019), art. No. 165453.
- [3] R.A. Sharma, Neodymium production processes, *JOM*, 39(1987), No. 2, p. 33.
- [4] E. Stefanidaki, C. Hasiotis, and C. Kontoyannis, Electrodeposition of neodymium from LiF–NdF₃–Nd₂O₃ melts, *Electrochim. Acta*, 46(2001), No. 17, p. 2665.
- [5] H.M. Zhu, Rare earth metal production by molten salt electrolysis, [in] G. Kreysa, K. Ota, and R.F. Savinell, eds., *Encyclopedia of Applied Electrochemistry*, Springer, New York, 2014, p. 1765.
- [6] G.H. Wang, X.S. Wang, and H.M. Zhu, Electroanalytical study of electrode processes on carbon anode in lithium fluoride and neodymium fluoride melt, *J. Rare Earths*, 25(2007), Suppl. 1, p. 533.
- [7] S.S. Nissen and D.R. Sadoway, Perfluorocarbon (PFC) generation in laboratory-scale aluminum reduction cells, [in] *Light Metals: Proceedings of Sessions*, TMS Annual Meeting, Orlando, 1997, p. 159.
- [8] F.M. Kimmeler, G. Potvin, and J.T. Pisano, Measured versus calculated reduction of the PFC emissions from prebaked Hall Héroult cells, [in] *Light Metals: Proceedings of Sessions*, TMS Annual Meeting, Orlando, 1997, p. 165.
- [9] H.M. Zhu and D.R. Sadoway, An electroanalytical study of electrode reactions on carbon anodes during electrolytic production of aluminum, [in] *Light Metals: Proceedings of Sessions*, TMS Annual Meeting, Nashville, 2000, p. 257.
- [10] H. Vogel and B. Friedrich, Reducing greenhouse gas emission from the neodymium oxide electrolysis. Part II: Basics of a process control avoiding PFC emission, *Int. J. Nonferrous Metall.*, 6(2017), No. 3, p. 27.
- [11] S.Z. Liu, L.Y. Chen, B. Li, L.L. Wang, B. Yan, and M.G. Liu, Anode processes for Nd electrowinning from LiF–NdF₃–Nd₂O₃ melt, *Electrochim. Acta*, 147(2014), p. 82.
- [12] B. Li, S.Z. Liu, H. Wang, and Z.X. Zhao, Electrochemistry for Nd electrowinning from fluoride-oxide molten salts, [in] N.R. Neelameggham, S. Alam, H. Oosterhof, A. Jha, and S.J. Wang, eds., *Rare Metal Technology 2014*, John Wiley & Sons, Inc., Hoboken, New Jersey, 2014, p. 95.
- [13] H. Imoto, K. Ueno, and N. Watanabe, A study on the anode effect in KF–2HF System. III. Influence of bath temperature and surface tension and addition of fluoride particles on the occurrence of the anode effect, *Bull. Chem. Soc. Jpn.*, 51(1978), No. 10, p. 2822.
- [14] L. Bai and B.E. Conway, Electrochemistry of anodic fluorine gas evolution at carbon electrodes: Part II studies on the ‘CF’ film by the current-interruption, AC impedance, ESCA and auger techniques, *J. Appl. Electrochem.*, 20(1990), No. 6, p. 916.
- [15] G. Chen, Z.N. Shi, Z.W. Wang, J.Y. Yu, J.L. Xu, X.W. Hu, B.L. Gao, and A.M. Liu, Mechanism of graphite electrode fluorinated in 2.4NaF/AlF₃–Al₂O₃ melt at 1373 K, *J. Electrochem. Soc.*, 161(2014), No. 14, p. C587.
- [16] Y. Castrillejo, P. Fernández, M.R. Bermejo, E. Barrado, and A.M. Martínez, Electrochemistry of thulium on inert electrodes and electrochemical formation of a Tm–Al alloy from molten chlorides, *Electrochim. Acta*, 54(2009), No. 26, p. 6212.